CHEMNANOMAT

CHEMISTRY OF NANOMATERIALS FOR ENERGY, BIOLOGY AND MORE

www.chemnanomat.org

Accepted Article

Title: Supramolecular Assembly of Thiolated Cyclodextrin and Ferrocene Derivative for Controlled Drug Delivery

Authors: Jian-Guang Cheng, Ying-Ming Zhang, and Yu Liu

To be cited as: *ChemNanoMat* 10.1002/cnma.201800098

Link to VoR: http://dx.doi.org/10.1002/cnma.201800098

A Journal of

ACES Asian Chemical Editorial Society

A sister journal of **Chemistry – An Asian Journal** and **Asian Journal of Organic Chemistry**

WILEY-VCH

COMMUNICATION WILEY-VCH

Supramolecular Assembly of Thiolated Cyclodextrin and Ferrocene Derivative for Controlled Drug Delivery

Jian-Guang Cheng,[a] Ying-Ming Zhang,[a] and Yu Liu*[a],[b]

Abstract: Construction of biocompatible nanoparticles is a significant topic of research at the chemistry–biology interface. Presently, more and more researchers have focused on supramolecular amphiphiles constructed by macrocycle-induced aggregation, a feasible and universal strategy in the fabrication of functional nanomaterials. In this work, we report a pH-responsive nanoparticle through the noncovalent complexation between per-6-thiolated β-cyclodextrin sodium salt (**SACD**) and amphiphilic ferrocene derivative (**$FC_{12}^{+}Br^{-}$**) in water. The formation and composition of the obtained supramolecular nanoparticles were comprehensively characterized by UV/Vis absorption, dynamic laser scattering, and microscopic observations. Furthermore, the drug loading and release studies demonstrated that the supramolecular binary nanoparticles could efficiently encapsulate doxorubicin hydrochloride (**DOX**) in their nanoparticulate cores, and the entrapped **DOX** could be rapidly released in the low pH environment. The present study suggests that the obtained binary supramolecular amphiphiles with good stability, tunable assembling/disassembling behaviors, and controlled drug loading/release properties have great potential in the construction of on-demand drug delivery systems.

Introduction

The emerging growth of supramolecular nanoparticles is considered as the innovative revolution for developing novel drug delivery systems in biomedical science, mainly due to their representative features of simplicity, versatility, and reversibility.[1] Several types of noncovalent interactions, such as hydrophobic,[2] hydrogen-bonding,[3] charge-transfer,[4] and π–π stacking interactions,[5] have been extensively used to tune the critical aggregation concentration (CAC), molecular amphiphilicity, and assembling modes of the building components, which can eventually affect the biological properties of resultant self-assembled nanostructures.[6] In this regard, the concept of macrocycle-induced aggregation, which is derived from the synergetic combination of macrocyclic hosts and amphiphilic guests, have been implemented as a smart and powerful strategy in the construction of various supramolecular nanoparticles, including functionalized micelles and vesicles in many biological fields.[7]

In the previous studies, it is demonstrated that the neutral cucurbiturils and sulfonated calixarenes are two main categories that can induce molecular aggregation of a variety of guest species, including fluorescent dyes,[8] amphiphilic surfactants,[9] and biological important molecules,[10] mainly through ion–diploe and electrostatic interactions.[11] These systems can be further endowed with multistimuli-responsive capability to develop as advanced drug delivery vehicles.[12] Compared to these frequently used macrocycles, the self-aggregation induced by cyclodextrins (CDs) was sporadically reported, which is probably due to the assumption that the conventional host–guest complexation in the hydrophobic cavity of CDs always prevent the amphiphilic guests from self-aggregation in aqueous media. Therefore, it is imperative to explore the CD-induced aggregation systems for practical bio-related application,[13] since CDs possess many fascinating physicochemical properties, such as good water-solubility, well-defined molecular structures, high biocompatibility, low-price commercial availability, and accessible chemical modification.[14]

In this work, we synthesized a per-6-substituted β-CD derivative possessing seven negative changes located on the upper rim (**SACD**), and the introduction of multiple carboxylate groups through a thioether linkage not only further increased the water solubility of β-CD, but also dramatically changed the molecular aggregation of amphiphilic guest. The amphiphilic guest used herein was ferrocene-derived quaternary ammonium salt bearing a dodecyl tail (**$FC_{12}^{+}Br^{-}$**), which could self-aggregate at a relatively higher concentration. It is noted that **$FC_{12}^{+}Br^{-}$** could be assembled as supramolecular nanoparticles with assistance of **SACD**, accompanied by the sharp decline of the CAC value of **$FC_{12}^{+}Br^{-}$**. Meanwhile, doxorubicin hydrochloride (**DOX**) as a model drug molecule could be encapsulated in the core of binary supramolecular nanoparticles, thus exhibiting pH-responsive drug release process under acidic condition (Scheme 1). This controlled molecular aggregation induced by negatively charged CDs may show practical possibilities in the construction of more advanced drug delivery systems.

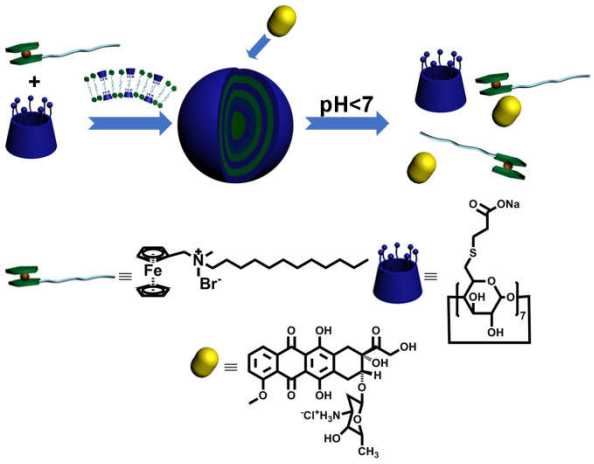

Scheme 1. Construction of a binary supramolecular nanoparticle based on **SACD** and **$FC_{12}^{+}Br^{-}$**.

Results and discussion

Characterization of Host−Guest Complexation in Water

As validated by Job plot, the inclusion complexation between **SACD** and **$FC_{12}^{+}Br^{-}$** gave 1:1 binding stoichiometry in water (Figure S1, Supporting Information). Meanwhile, the proton signals of **$FC_{12}^{+}Br^{-}$** (H_a) displayed obvious downfield shifts upon

[a] College of Chemistry, State Key Laboratory of Elemento-Organic Chemistry, Nankai University, Tianjin 300071, P. R. China
E-mail: yuliu@nankai.edu.cn
[b] Collaborative Innovation Center of Chemical Science and Engineering (Tianjin), Tianjin 300072, China
Supporting information for this article is given via a link at the end of the document.

addition of **SACD**, and the binding constant (K_S) of **$FC_{12}^+Br^-$**⊂**SACD** was accordingly calculated as (2.37 ± 0.34) × 10^4 M^{-1} in in 0.01 M phosphate buffer solution (pH = 7.2) at 25 °C by using nonlinear curve-fitting method (Figure S2, Supporting Information).[15] It is noteworthy that this obtained binding constant is much larger than that of positively charged ferrocene derivatives with native β-CD (*ca.* 10^3 $^{-1}$), which can be attributed to the synergetic electrostatic interaction from the multiple carboxylate groups in **SACD**.[16] In addition, as shown in the ROESY spectrum of an equimolar mixture of **$FC_{12}^+Br^-$** with **SACD**, the cross-peaks A were assigned to NOE correlations of ferrocene species of $FC_{12}^+Br^-$ with H3 protons of **SACD**, and the cross peaks B were assigned to the ones with H5 protons of **SACD**. The intensity of former NOE correlations seems relatively stronger than the latter ones. Moreover, considering that the intermolecular distance between quaternary ammonium site in **$FC_{12}^+Br^-$** and carboxylic site in **SACD** could be much closer to facilitate the mutual electrostatic interaction, we can reasonably deduce that the **$FC_{12}^+Br^-$** guest was included in the **SACD** cavity mainly from its lower rim (Figure S3, Supporting Information).

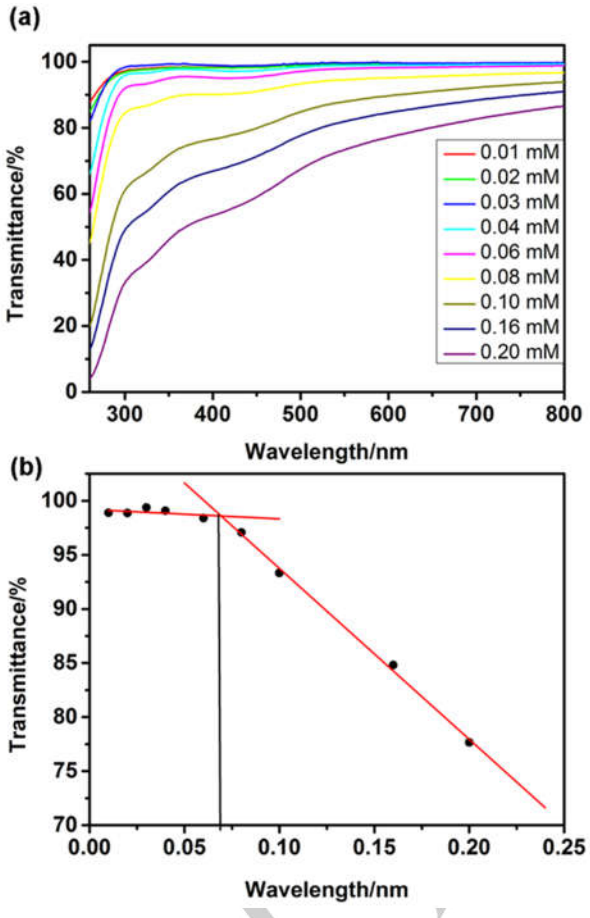

Figure 1. (a) Optical transmittance of aqueous solutions containing **SACD** (8.0 μM) upon addition of **$FC_{12}^+Br^-$** at different concentrations ([**$FC_{12}^+Br^-$**] = 0.01–0.20 mM) at 25 °C; (b) Dependence of optical transmittance at 500 nm versus the concentration of **$FC_{12}^+Br^-$**.

Cyclic voltammetry experiments were further carried out to study the electrochemical properties in **$FC_{12}^+Br^-$**⊂**SACD** complex. As compared to free **$FC_{12}^+Br^-$** in aqueous buffer solution, the anodic peak current of the inclusion complex was obviously decreased, originating from the relatively lower diffusion coefficient of **SACD**-bound **$FC_{12}^+Br^-$** than the unbound one (Figure S4, Supporting Information). Moreover, the half-wave potential was also decreased upon addition of **SACD**, accompanied by the one-electron oxidation of the ferrocene moiety, jointly suggesting that the oxidized form of **$FC_{12}^+Br^-$** could form a more stable inclusion complex with **SACD**.[17]

Construction and Characterization of Supramolecular Binary Nanoparticle

Considering the amphiphilic property of **$FC12^+Br^-$** and the favourable electrostatic attraction with multiple carboxylate groups in **SACD**, we next investigated the molecular aggregation behaviors of **SACD** and **$FC_{12}^+Br^-$** by monitoring the optical transmittance in UV/Vis spectroscopic experiments. The optical transmittance was recorded at 500 nm, because no appreciable change was observed in the concentration range from 0.005 to 0.2 mM for free **$FC_{12}^+Br^-$** (Figure S5, Supporting Information). In contrast, as shown in Figure 1, the critical aggregation concentration (CAC) of **$FC_{12}^+Br^-$**was dramatically decreased to 0.068 mM when the concentration of **SACD** was fixed at 8.0 μM, which was over 7 times lower than the one of free guest molecule (0.5 mM).[18]

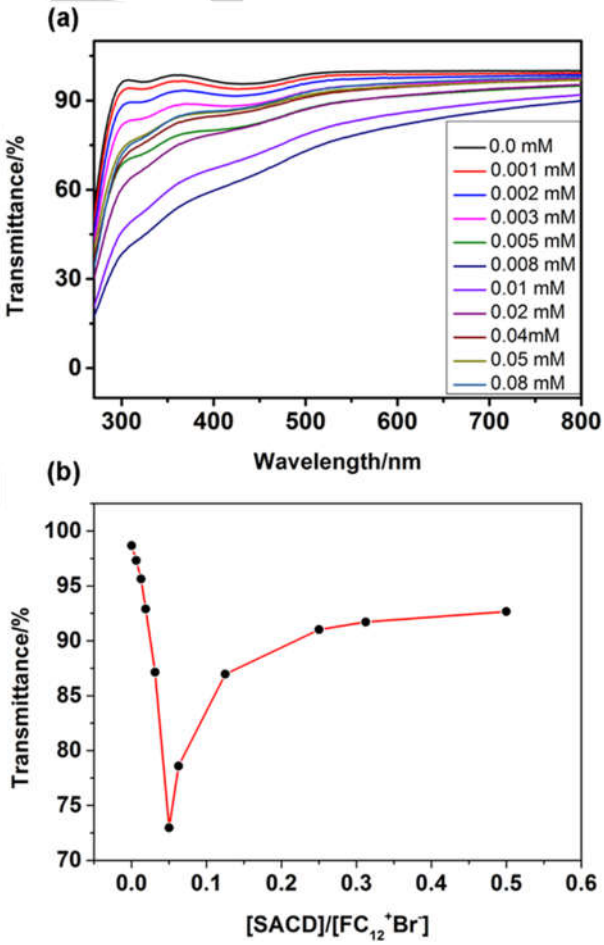

Figure 2. (a) Optical transmittance of **$FC_{12}^+Br^-$** (0.16 mM) by increasing the concentration of **SACD** from 0.0 to 0.08 mM at 25 °C in water. (b) Dependence of the optical transmittance at 500 nm on the **SACD** concentration with a fixed **$FC_{12}^+Br^-$** concentration of 0.16 mM at 25 °C.

Subsequently, the optimal molar ratio in the formation of binary nanoparticles was determined. When the concentration was fixed at 0.16 mM, the optical transmittance of **$FC_{12}^+Br^-$** at 500 nm gave a minimum value at the molar ratio of 0.05 upon continuous addition of **SACD** (Figure 2), suggesting that the best mixing ratio for the amphiphilic assembly was located at 1:20 **SACD**: **$FC_{12}^+Br^-$**. The decline of optical transmittance before this

point indicates the gradual formation of supramolecular amphiphilic aggregates, while the resultant assembly was eventually dissipated to simple inclusion complexes in the presence of excess amount of **SACD**. In our case, the aggregation of **$FC_{12}^{+}Br^{-}$** induced by the complexation of **SACD** may occur in two steps. First, the host and guest molecules instantaneously formed simple inclusion complexes driven by the hydrophobic and electrostatic interactions. Next, the additional **$FC_{12}^{+}Br^{-}$** molecules were readily integrated into these supramolecular complexes, which eventually resulted in the formation of compact binary nanoaggregates (Scheme 1).

Compared to free **$FC_{12}^{+}Br^{-}$**, a simple mixture of **SACD** (8.0 μM) and **$FC_{12}^{+}Br^{-}$** (0.16 mM) showed a clear Tyndall effect, indicative of abundant aggregates formed in the solution (Figure 3a, inset). Meanwhile, the dynamic laser scattering (DLS) and transmission electron microscopic (TEM) experiments were carried out to comprehensively identify the size and morphology of this binary supramolecular nanoparticle. The DLS result showed that the nanoparticle possessed a narrow size distribution with an average diameter of 206 nm at a scattering angle of 90°. Accordingly, the formation of nanoparticle was convincingly validated by TEM investigation, showing the solid particulate morphology with an average diameter of 180 nm, which was basically consistent with the DLS results. Furthermore, Zeta potential was measured as –77.67 mV, implying that the electrostatic force is an indispensable factor to maintain the overall stability of the supramolecular nanoaggregates (Figure 3a). Meanwhile, the stability of the binary nanoparticles was investigated by monitoring the optical transmittance at 500 nm in 24 h (Figure 4). No appreciable change in the optical transmittance was observed in this period of time, here again corroborating the stability of the obtained nanoparticle.

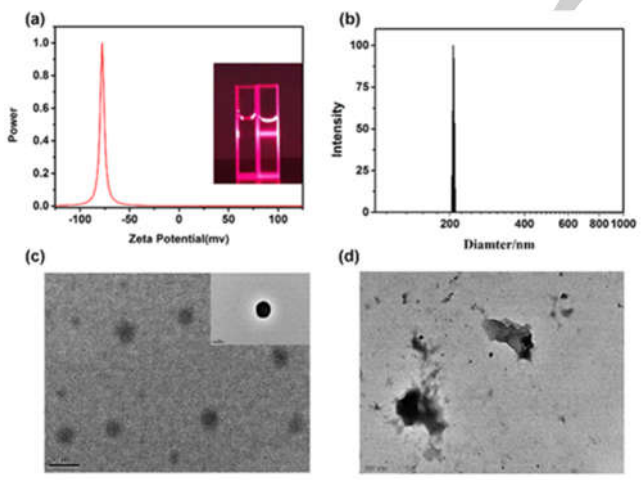

Figure 3. (a) Zeta potential, (b) DLS data, (c) TEM image of **SACD** + **$FC_{12}^{+}Br^{-}$** assembly, scale bar=200 nm; (d) TEM image of the **SACD** + **$FC_{12}^{+}Br^{-}$** assembly after adjusting the pH of the solution to 4.0, scale bar=500 nm; [**SACD**] = 8.0 μM, and [**$FC_{12}^{+}Br^{-}$**] = 0.16 mM. Inset in (a): Tyndall effect of free **$FC_{12}^{+}Br^{-}$** solution (left) and **SACD** + **$FC_{12}^{+}Br^{-}$**aggregate (right).

The electrostatic interaction between **SACD** and **$FC_{12}^{+}Br^{-}$** enabled us to adjust the stimuli-responsive behaviors of binary nanoparticles by varying the pH values. As expected, the obtained supramolecular nanoparticles were disassembled under acidic condition (pH 4.0), mainly due to the protonation of carboxylic sites in the host compound. On the contrary, the supramolecular nanoparticles were re-assembled under neutral condition (pH 7.5). This reversible pH-responsive behavior could be conveniently observed by the optical transmittance of the nanoparticle at pH 4.0 and 7.5, respectively (Figure 5). The good cycling performance under acidic and neutral conditions may further facilitate the pH-triggered drug release, as discussed below.

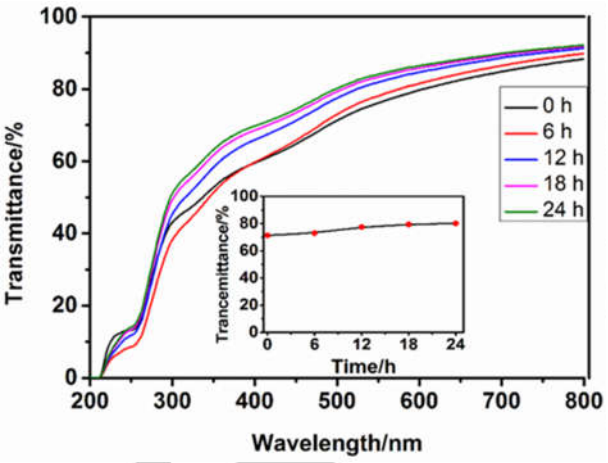

Figure 4. Optical transmittance of **SACD** + **$FC_{12}^{+}Br^{-}$** assembly within 24 h at 25 °C. ([**SACD**] = 8.0 μM and [**$FC_{12}^{+}Br^{-}$**] = 0.16 mM). Inset: the change of optical transmittance at 500 nm versus time.

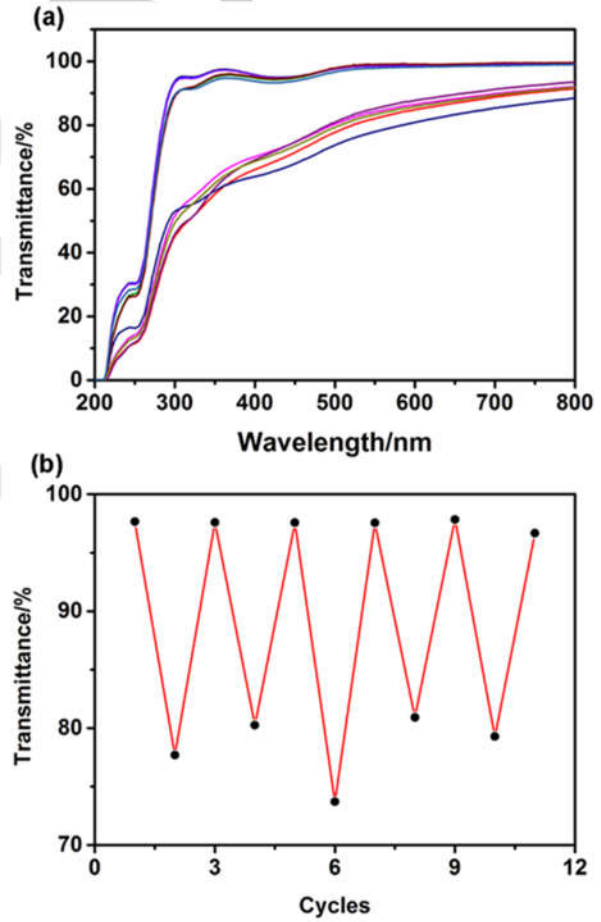

Figure 5. (a) Optical transmittance of the **SACD** + **$FC_{12}^{+}Br^{-}$** assembly at different pH values; (b) Dependence of the optical transmittance of the **SACD** + **$FC_{12}^{+}Br^{-}$** assembly at 500 nm with varying pH at 4.0 and 7.5, respectively ([**SACD**] = 8.0 μM, [**$FC_{12}^{+}Br^{-}$**] = 0.16 mM).

Drug loading and pH-triggered release

It is reasonable to expect that the pH-responsive assembly **SACD** and **$FC_{12}^{+}Br^{-}$** could load drug molecule into its nanoparticulate interiors and then release drug molecule when the nanoparticles were disassembled. In our case, doxorubicin hydrochloride (**DOX**) was chosen as the model drug molecule. Drug-loaded nanoparticles were fabricated by adding **DOX**

solution into a freshly prepared aqueous solution of **SACD** (8.0 μM) and **FC$_{12}$$^{+}$Br^{-}** (0.16 mM), and unloaded **DOX** molecules were removed by dialysis against water. Compared to the non-loaded nanoparticles, **DOX**-loaded ones showed board absorption ranging from 400 to 550 nm, which could be clearly assigned to the UV/Vis absorption of **DOX** (Figure 6a). Besides, the solution colour instantly turned red after loading **DOX** into binary supramolecular nanoparticles (Figure 6a, inset). Furthermore, according to UV titration results, the DOX encapsulation efficiency was calculated to be 9.8%.

The release behaviors of **DOX** at different pH value were investigated by means of fluorescence emission spectroscopy. As shown in Figure 6b, a very low release rate of **DOX** was observed over a period of 100 min at pH 7.5, indicating that the drug-loaded assembly was highly stable at room temperature in aqueous medium under neutral condition. In contrast, the release rate was significantly enhanced when the solution was adjusted to pH 4.0 and 6.5. Under acidic condition, more than 60% and 90% **DOX** were released at pH 6.5 and 4.0, respectively, within 150 min. These rapid drug release behaviors showed a good responsivity toward the change of pH values, thus making **DOX**-loaded nanoparticles a promising candidate for efficient drug delivery.

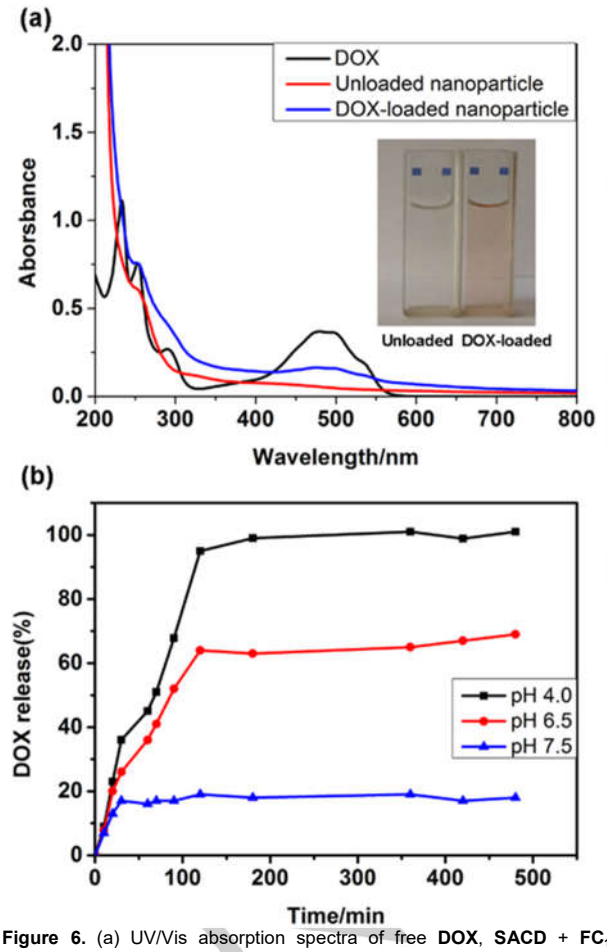

Figure 6. (a) UV/Vis absorption spectra of free **DOX**, **SACD** + **FC$_{12}$$^{+}$Br^{-}** assembly, and **DOX**-loaded assembly at 25 °C in water. Inset: colour change of **SACD** + **FC$_{12}$$^{+}$Br^{-}** assembly (left) and **DOX**-loaded assembly (right). (b) Release of **DOX** entrapped in the **SACD** + **FC$_{12}$$^{+}$Br^{-}** assembly at different pH values.

Conclusion

In summary, by utilizing the molecular induced aggregation strategy, we have successfully constructed a supramolecularly amphiphilic system through the noncovalent binding between alkyl chain-modified ferrocene derivative (**FC$_{12}$$^{+}$Br^{-}**) and multiply charged β-cyclodextrin (**SACD**). Remarkably, the critical aggregation concentration of amphiphilic ferrocene ammonium salt was dramatically decreased by *ca.* 7.4 times upon association with **SACD**. More gratifyingly, the disassembling of binary supramolecular assembly and the release of entrapped drug molecules can be conveniently realized under acidic condition. Thus, considering the intrinsic acidic environment in most of tumor cells, we can anticipate that this work may promote the multiply charged cyclodextrins as intelligent macrocyclic receptors to enhance the drug loading efficiency and achieve specific release at action sites in cancer treatments.

Experimental Section

Materials

I_2, PPh_3 was purchased from HEWONS, and 3-sulfanylpropionic acid was purchased from TCI. All of these were used without further purification.β-Cyclodextrin (β-CD, Kermel, China) was purified twice by recrystallization from water before use. *N*,*N*'-Dimethylformamide was stirred overnight with CaH2 and distilled under reduced pressure prior to use. Acetonitrile was stirred overnight with CaH_2 and distilled prior to use. Doxorubicin hydrochloride (**DOX**) was purchased from Knowshine (Shanghai) Pharmachemicals Inc. (Shanghai, China). Heptakis-[6-deoxy-6-(3-sulfanylpropanoic acid)]-β-cyclodextrin (**SACD**) and ferrocene derivative (**FC$_{12}$$^{+}$Br^{-}**) was synthesized and purified according to the previous literatures.[19]

UV-Vis spectroscopy

UV-Vis spectra and the optical transmittance were recorded in a quartz cell on a Shimadzu UV-3600 spectrophotometer equipped with a PTC-348WI temperature controller.

Fluorescence spectroscopy

Fluorescence spectra were recorded in a conventional quartz cell (light path 10 mm) on a Varian Cary Eclipse equipped with a Varian Cary single-cell Peltier accessory to control the temperature.

TEM

TEM images were recorded on a Tecnai 20 high-resolution transmission electron microscope operating at an accelerating voltage of 200 kV.

DLS

The sample solution for DLS measurement was prepared by filtering solution through a 200 nm Millipore filter into a clean scintillation vial. The sample solution for DLS measurement was prepared by filtering solution through a 200 nm Millipore filter into a clean scintillation vial. The samples were examined on a laser light scattering spectrometer (BI-200SM) equipped with a digital correlator (TurboCorr) at 636 nm at a scattering angle of 90. Zeta potential was measured on a Zeta PALS + BI-90 instrument (Brookhaven Co. USA).

DOX-loaded nanoparticle

The nanoparticles were prepared as follows: A certain amount of **DOX** was added to a solution containing **SACD** and **FC$_{12}$$^{+}$Br^{-}**, and then water was added until the volume of the solution reached 30 mL. The ultimate concentrations of **DOX**, **SACD** and **FC$_{12}$$^{+}$Br^{-}** were 0.2, 0.16, and 0.008 mM, respectively. Then the prepared **DOX**-loaded nanoparticles were purified by dialysisin distilled water for several times until the water outside the dialysis tube exhibited negligible **DOX** fluorescence emission.

The **DOX** encapsulation efficiency was calculated by the following equation:

Encapsulation efficiency (%) = (m_{loaded} /m_D) × 100

where m_{loaded} and m_D are mass of **DOX** encapsulated in the nanoparticle and mass of **DOX** added, respectively. The mass of **DOX** was measured by a UV spectrophotometer at 482 nm.

Acknowledgements

We thank the National Natural Science Foundation of China (Nos. 21432004, 21472100, 21772099, and 91527301) for financial support.

Keywords: Cyclodextrin • Ferrocene • pH-responsiveness • Supramolecular nanoparticle • Molecular Aggregation

[1] Y. Wang, H. Xu, X. Zhang, *Adv. Mater.* **2009**, *21*, 2849–2864.
[2] a) J. W. Barnett, B. C. Gibb, H. S. Ashbaugh, *J. Phys. Chem. B* **2016**, *120*, 10394–10402; b) B. H. Northrop, A. Glöckner, P. J. Stang, *J. Org. Chem.* **2008**, *73*, 1787–1794.
[3] a) N. Kimizuka, T. Kawasaki, K. Hirata, T. Kunitake, *J. Am. Chem. Soc.***1998**,*120*, 4094–4104; b) Y. Chen, A. M. Kushner, G. A. Williams, Z. Guan, *Nat. Chem.* **2012**, *4*, 467–472.
[4] D.-Q. Yuan, A. Izuka, M. Fukudome, M. V. Rekharsky, Y. Inoue, K. Fujita, *Tetra. Lett.* **2007**, *48*, 3479–3483.
[5] a) S. Burattini, B. W. Greenland, D. H. Merino, W. Weng, J. Seppala, H. M. Colquhoun, W. Hayes, M. E. Mackay, I. W. Hamley, S. J. Rowan, *J. Am. Chem. Soc.* **2010**, *132*, 12051–12058; b) A. Feng, L. Peng, B. Liu, S. Liu, S. Wang, J. Yuan, *ACS Appl. Mater. Interfaces* **2016**, *8*, 11024–11030.
[6] a) D.-S. Guo, K. Wang, Y.-X. Wang, Y. Liu, *J. Am. Chem. Soc.* **2012**, *134*, 10244–10250; b) T. Ogoshi, M. Hashizume, T.-a. Yamagishi, Y. Nakamoto, *Langmuir* **2010**, *26*, 3169–3173; c) D. Zhao, Y. Chen, Y. Liu, *Chem. Asian J.* **2014**, *9*, 1895–1903.; d) J. Wu, C. Gao, *Macromolecules* **2010**, *43*, 7139–7146.
[7] a) F. Sallas, R. Darcy, *Eur. J. Org. Chem.* **2008**, 957–969; b) V. Wintgens, C. Le Coeur, C. Amiel, J.-M. Guigner, J. G. Harangozó, Z. Miskolczy, L. Biczók, *Langmuir* **2013**, *29*, 7682–7688; c) Y.-W. Yang, Y.–L. Sun, N. Song, *Acc. Chem. Res.* **2014**, *47*, 1950–1960; d) Q. Zeng, R. Marthi, A. McNally, C. Dickinson, T. E. Keyes, R. J. Forster, *Langmuir* **2010**, *26*, 1325–1333; e) M.-X. Wu, Y.-W. Yang, *Adv. Mater.* **2017**, 29, 1606134; f) Z. Li, Y.-W. Yang, *J. Mater. Chem. B* **2017**, 5, 9278–9290.
[8] a) L. A. Baumes, M. Buaki, J. Jolly, A. Corma, H. Garcia, *Tetrahedron Letters* **2011**, *52*, 1418–1421; b) M. Florea, W. M. Nau, *Angew. Chem. Int. Ed.* **2011**, *50*, 9338-9342; *Angew. Chem.* **2011**, 123, 9510–9514.
[9] N. Basilio, L. García-Río, *Chem. Eur. J.* **2009**, *15*, 9315–9319.
[10] D.-S. Guo, Y. Liu, *Acc. Chem. Res.* **2014**, *47*, 1925–1934.
[11] W. Tao, M. Barra, *J. Org. Chem.* **2001**, *66*, 2158–2160.
[12] V. C. Özalp, T. Schäfer, *Chem. Eur. J.* **2011**, *17*, 9893-9896.
[13] T. Loftsson, M. E. Brewster, *J. Pharm. Sci.* **2012**, *101*, 3019–3032.
[14] a) J. Szejtli, *Chem. Rev.* **1998**, *98*, 1743–1754; b) K. Uekama, F. Hirayama, T. Irie, *Chem. Rev.* **1998**, *98*, 2045–2076; c) J. M. Haider, Z. Pikramenou, *Chem. Soc. Rev.* **2005**, *34*, 120–132; d) A. Martinez, C. Ortiz Mellet, J. M. Garcia Fernandez, *Chem. Soc. Rev.* **2013**, *42*, 4746–4773; e) F. Sallas, R. Darcy, *Eur.J.Org.Chem.* **2008**, *2008*, 957–969.
[15] J. Ma, H. Deng, S. Ma, J. Li, X. Jia, C. Li, *Chem. Comm.* **2015**, *51*, 6621–6624.
[16] a) F. M. Menger, M. J. Sherrod, *J. Am. Chem. Soc.* **1988**, *110*, 8606–8611; b)R. Breslow, M. F. Czarniecki, J. Emert, H. Hamaguchi, *J. Am. Chem. Soc.* **1980**, *102*, 762–770; c)W. S. Jeon, K. Moon, S. H. Park, H. Chun, Y. H. Ko, J. Y. Lee, E. S. Lee, S. Samal, N. Selvapalam, M. V. Rekharsky, V. Sindelar, D. Sobransingh, Y. Inoue, A. E. Kaifer, K. Kim, *J. Am. Chem. Soc.* **2005**, *127*, 12984–12989.
[17] a) Y. Liu, R. Cao, Y. Chen, J.-Y. He, *J. Phys. Chem. B* **2008**, *112*, 1445–1450; b)Q. Duan, Y. Cao, Y. Li, X. Hu, T. Xiao, C. Lin, Y. Pan, L. Wang, *J. Am. Chem. Soc.* **2013**, *135*, 10542–10549.
[18] T. Saji, K. Hoshino, S. Aoyagui, *J. Am. Chem. Soc.* **1985**, *107*, 6865–6868.
[19] a) R. Isnin, C. Salam, A. E. Kaifer, *J.Org. Chem.* **1991**, 56, 35–41. b)A. Bom, M. Bradley, K. Cameron, J. K. Clark, J. van Egmond, H. Feilden, E. J. MacLean, A. W. Muir, R. Palin, D. C. Rees, M.-Q. Zhang, *Angew. Chem. Int. Ed.* **2002**, *41*, 265–270; *Angew. Chem.* **2002**, *114*, 275–280

.

Entry for the Table of Contents

COMMUNICATION

In this work, a pH-responsive supramolecular nanoparticle with good stability, tunable assembling/disassembling behaviors, and controlled drug loading/release properties was reported, which make it applealing for the construction of controlled drug delivery systems.

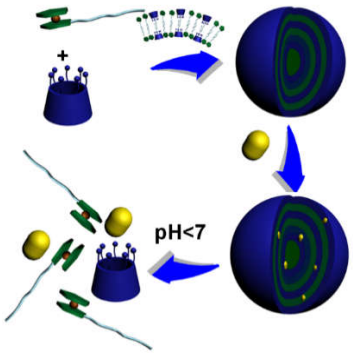

*Jian-Guang Cheng, Ying-Ming Zhang, and Yu Liu**

Supramolecular Assembly of Thiolated Cyclodextrin and Ferrocene Derivative for Controlled Drug Delivery